



Validation of a simple model to predict the performance of methane oxidation systems, using field data from a large scale biocover test field



Christoph Geck^{a,*}, Heijo Scharff^b, Eva-Maria Pfeiffer^a, Julia Gebert^a

^aUniversität Hamburg, Institute of Soil Science, Allende-Platz 2, 20146 Hamburg, Germany

^bNV Afvalzorg Holding, Nauerna 1, 1566 PB Assendelft, The Netherlands

ARTICLE INFO

Article history:

Received 18 March 2016

Revised 20 May 2016

Accepted 6 June 2016

Available online 12 July 2016

Keywords:

Landfill cover soil

Landfill gas

Model validation

Flux chamber

Spatial variability

Temporal variability

ABSTRACT

On a large scale test field (1060 m²) methane emissions were monitored over a period of 30 months. During this period, the test field was loaded at rates between 14 and 46 g CH₄ m⁻² d⁻¹. The total area was subdivided into 60 monitoring grid fields at 17.7 m² each, which were individually surveyed for methane emissions and methane oxidation efficiency. The latter was calculated both from the direct methane mass balance and from the shift of the carbon dioxide - methane ratio between the base of the methane oxidation layer and the emitted gas. The base flux to each grid field was back-calculated from the data on methane oxidation efficiency and emission. Resolution to grid field scale allowed the analysis of the spatial heterogeneity of all considered fluxes. Higher emissions were measured in the upslope area of the test field. This was attributed to the capillary barrier integrated into the test field resulting in a higher diffusivity and gas permeability in the upslope area. Predictions of the methane oxidation potential were estimated with the simple model Methane Oxidation Tool (MOT) using soil temperature, air filled porosity and water tension as input parameters. It was found that the test field could oxidize 84% of the injected methane. The MOT predictions seemed to be realistic albeit the higher range of the predicted oxidations potentials could not be challenged because the load to the field was too low. Spatial and temporal emission patterns were found indicating heterogeneity of fluxes and efficiencies in the test field. No constant share of direct emissions was found as proposed by the MOT albeit the mean share of emissions throughout the monitoring period was in the range of the expected emissions.

© 2016 Elsevier Ltd. All rights reserved.

1. Introduction

Methane oxidation systems (MOS) were shown to be capable of remediating residual methane fluxes from landfills following the period of technical treatment and are considered an important tool of secondary control of landfill methane emissions (Bogner et al., 2007). Various studies have been carried out to quantify the methane oxidation capacity of soils under different conditions in the laboratory and on-site (overview in (Scheutz et al., 2009). Optima for environmental conditions (Park et al., 2009; Scheutz and Kjeldsen, 2004; Stein and Hettiaratchi, 2001)) and recommendations regarding the employed soil material (LAGA Ad-hoc AG “Deponietechnik”, 2011) were derived. However, especially for methane oxidation covers (also called biocovers) several problems exist regarding on-site quantification of performance: (1) gas gen-

eration and therefore flux to the cover is usually not known; (2) microbial communities are a dynamic component of soils, on the one hand capable of adaptation to changing environmental conditions and on the other hand prone to environmental stresses like for example drought, extreme temperatures or low nutrient availability. The result is a high temporal variability of emissions (Rachor et al., 2013; Teclé et al., 2009). (3) Due to inhomogeneity of the soil with respect to its physical parameters like bulk density, aggregate structure or moisture distribution and corresponding properties such as air-filled porosity, diffusivity and gas permeability, the spatial pattern of substrate delivery to the microorganisms and of environmental conditions vary. Hence, oxidation rates are also subject to high spatial variability (Bogner et al., 1997; Rachor et al., 2013; Röwer et al., 2011; Teclé et al., 2009). Realistic assessment of larger areas requires an intensive measurement effort with a high areal coverage.

To improve knowledge of the behavior of field scale MOS a test field intended to simulate a methane oxidation cover was constructed in The Netherlands on a site of NV Afvalzorg and monitored about monthly over a period of 30 months. The test field

* Corresponding author.

E-mail addresses: christoph.geck@uni-hamburg.de (C. Geck), h.scharff@afvalzorg.nl (H. Scharff), eva-maria.pfeiffer@uni-hamburg.de (E.-M. Pfeiffer), julia.gebert@ifb.uni-hamburg.de (J. Gebert).

was loaded with methane up to $56 \text{ g m}^{-2} \text{ d}^{-1}$. Sites with a gas generation of up to $35 \text{ g m}^{-2} \text{ d}^{-1}$ are considered suitable for methane oxidation application in the view of the operator NV Afvalzorg. Hence the load to the test field was above the expected loads in real application. For this study, retrieved data was compared to the predictions of the application model *Methane Oxidation Tool (MOT)*, Gebert et al., 2011c) designed for the estimation of efficiencies of MOS. The purpose was to test whether the model assumptions on the environmental process drivers (air-filled porosity, temperature, water tension) and on the share of the load to the cover soil bypassing the soil as direct emissions (i.e. hotspot-emissions) result in realistic predictions of MOS efficiencies. An additional focus was set on the spatial variability of oxidation efficiencies.

2. Material and methods

2.1. Setup and operation of test field

The test field was situated on a 1:5 sloped edge of a landfill in the northwest of The Netherlands. The field had a size of 1060 m^2 and was integrated into the landfill top cover but separated from the waste body by a high density polyethylene (HDPE) membrane so that only the purposely injected gas entered the test field. Gas injection was realized by six inlet ports situated on the HDPE base sealing within the catchment area that was built to monitor the water infiltration regime of the test field (Figs. 1 and 2). The catchment was delimited with a 40 cm HDPE border welded perpendicularly to the base sealing. The gas supplied to the field at a controllable rate was extracted from two nearby gas wells and monitored with respect to gas quality and quantity and the data were logged in an interval of 10 min. During the investigation period, the inlet flux was varied between 0.7 and $2.6 \text{ m}^3 \text{ CH}_4 \text{ h}^{-1}$, corresponding to a nominal load to the test field of $10\text{--}57 \text{ g CH}_4 \text{ m}^{-2} \text{ d}^{-1}$, assuming even spatial distribution of the base flux. Three flux levels were investigated: $37.8 \text{ g CH}_4 \text{ m}^{-2} \text{ d}^{-1} \pm 8.4$ from August 2012 until July 2013, $13.7 \text{ g CH}_4 \text{ m}^{-2} \text{ d}^{-1} \pm 2.1$ from February 2014 until May 2014 and $46.4 \text{ g CH}_4 \text{ m}^{-2} \text{ d}^{-1} \pm 8.3$ from August 2014 until February 2015 (Fig. 5).

The investigated MOS consisted of a capillary barrier (capillary block: 20 cm gravel (2–8 mm), capillary layer: 30 cm sand (1–2 mm)) and a methane oxidation layer (topsoil: 20 cm loam (according to *World reference base for soil resources (WRB)* (FAO, 2014): L), subsoil: 80 cm loamy sand (WRB: SL) (Fig. 1).

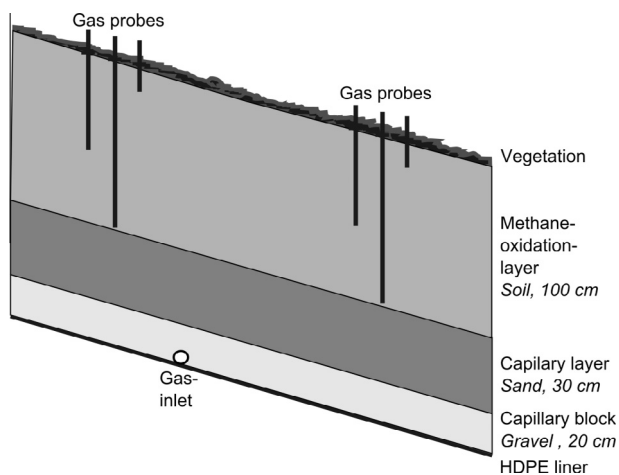


Fig. 1. Setup of test field, cross section.

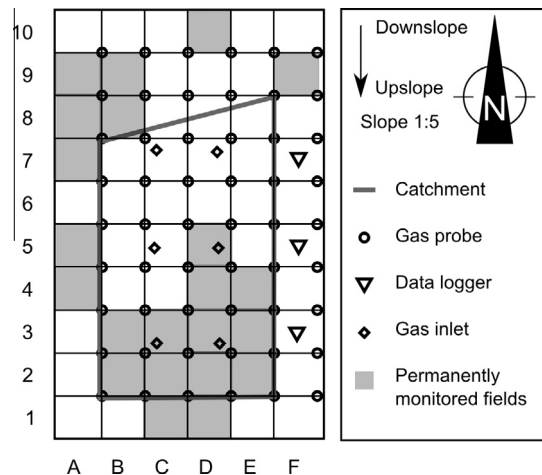


Fig. 2. Top view of test field. A1 to F10: grid fields for emission and soil gas concentration measurement. Grid size is $4.25 \text{ m} \times 4.25 \text{ m}$. Figure shows sampling scheme employed from August 2012 to July 2013: shaded fields monitored in each campaign, one third of white fields monitored per rotation every third campaign.

oxidation layer was initially constructed with a long stick excavator to avoid soil compaction. In July 2013 the test field was reconstructed. The upper 60 cm of the field were excavated and refilled using a bulldozer instead of a long stick excavator. This was done to achieve a higher degree of compaction and to assess the effects of standard construction practice on the relevant soil parameters and on system performance.

The capillary block was meant to function as gas distribution layer, distributing the gas over the entire base area of the test field before it moves upwards evenly through the oxidation layer.

On the surface of the test field a grid was marked permanently with pegs. The grid fields had a size of $4.25 \text{ m} \times 4.25 \text{ m}$. The grid was used to ensure a consistent positioning of the static chamber used for the emission measurement (see Section 2.2, Fig. 2). Also, the soil gas probes were aligned according to the grid (see Section 2.3).

In order to assess the soil environmental parameters relevant for the methane oxidation process, soil moisture (EC5, Decagon) and soil temperature probes (Pt1000) were installed 40 cm below surface in one downslope, one midslope and one upslope position (Fig. 2). Data of midday of each campaign were averaged from down-, mid- and upslope probe.

2.2. Measurement of emissions and campaigning strategy

Emissions were measured using a large static chamber. The quadratic chamber had a base area of 17.7 m^2 and a volume of 8.8 m^3 . It was constructed from an aluminum frame covered with aluminum coated plastic foil. Two fans inside of the chamber were mixing the air during the measurement. Gas was sampled continuously through 18 evenly distributed tubes and the change in methane concentration within the chamber over time was detected and recorded with a mobile flame ionization detector ((FID) Toxic Vapor Analyzer, Thermo Scientific, detection limit for methane: 0.25 ppm). Carbon dioxide concentration was recorded using a non-dispersive infrared (NDIR)-sensor (TSI, IAQ-CALC, Model 7525, detection limit for carbon dioxide 1 ppm) sampling the same gas stream as did the FID. Time of enclosure was four minutes. Details on the chamber setup and method validation are given in Geck et al. (2016). The grid fields covered by emission measurements were selected after a campaign in which all 60 grid fields of $4.25 \text{ m} \times 4.25 \text{ m}$ were measured. The fields accounting for 90% of the total methane emission were selected to be measured in

each campaign (permanently monitored fields, example in Fig. 2). One third of the remaining fields (equivalent to 3% of overall emissions) was measured each third campaign. Assuming a spatially stable emission pattern, the grid fields measured in each campaign summed up to 93% of overall methane emissions.

2.3. Measurement of soil gas composition

Composition of the soil gas phase was monitored by means of permanently installed gas probes on the aforementioned fixed grid with a cell size of 4.25 m × 4.25 m (Fig. 2). The probes were installed to 1 m depth which is the lower part of the methane oxidation layer. The probes consisted of aluminum tubes with an inner diameter of 7 mm. They were closed with butyl rubber stoppers and sampled by means of a 60 ml syringe. First, the inner volume of the gas probe was extracted and discarded, then a 60 ml sample was taken and analyzed immediately on site with a portable biogas analyser (BM 2000 “Biogas”, Geotechnical Instruments (UK) Ltd.) for the content of methane, carbon dioxide and oxygen. The accuracy of the device was 0.1% v/v per individual gas. Nitrogen content was calculated as balance to 100% as the landfill gas did not contain any other component in a relevant concentration, verified by a gas chromatographic analysis of the gas in May 2013.

2.4. Calculation of methane oxidation efficiency and base flux

To calculate the efficiency of the MOS, two approaches were used. (1) A direct methane mass balance was calculated by comparing the total ingoing CH₄ flux, known from the mass flow meter measurements in the test field gas injection system, to the total emitted CH₄ flux as assessed from the flux box measurements. This approach is straightforward but can assess the test field performance only “in bulk” without showing spatial variability of base fluxes and oxidation rates.

(2) The approach herein named carbon shift method was derived by Gebert et al. (2011b) and Christophersen et al. (2001) from the fact that the ratio of carbon dioxide and methane shifts with the oxidation process while the total volume of carbon dioxide and methane remains constant. They proposed that oxidation efficiency can be derived from the shift of the CO₂-CH₄ ratio when concentrations in the raw landfill gas and in a depth of interest are known (Eq. (1)). The carbon shift approach is robust against dilution by diffusive air ingress from the surface because both components are diluted to the same extent.

$$Eff_{Ox} = \frac{x}{CH_{4_LFG}} \times 100 \quad (1)$$

$$\text{with: } \frac{CO_{2_LFG} + x}{CH_{4_LFG} - x} = \frac{CO_{2_i}}{CH_{4_i}} \iff x = \frac{\frac{CO_{2_i}}{CH_{4_i}} \times CH_{4_LFG} - CO_{2_LFG}}{1 + \frac{CO_{2_i}}{CH_{4_i}}}$$

with

- Eff_{Ox} = Oxidation efficiency (% of inlet methane),
- CO_{2_LFG} = CO₂ concentration in landfill gas (vol.%),
- CH_{4_LFG} = CH₄ concentration in landfill gas (vol.%),
- CO_{2_i} = CO₂ concentration in depth i (vol.%),
- CH_{4_i} = CH₄ concentration in depth i (vol.%),
- x = Share of oxidized methane (fraction of 1).

Using this approach it is assumed that carbon dioxide production from soil respiration is negligible compared to carbon dioxide production from methane oxidation, that gas migration is vertical, i.e. that the methane and carbon dioxide concentrations measured in the emitted gas spatially relate to the concentrations at the base of the MOS below the point of the emission measurement and that the system is in a steady state. Using the carbon shift method the efficiency of the each grid field was calculated using the concentra-

tion in 1 m depth and the volumetric emissive flux of carbon dioxide and methane at the surface.

As base flux the influx to the particular grid field in 1 m depth was defined as this was the base of the methane oxidation layer and the methane and carbon dioxide concentration in 1 m depth was used to calculate its methane oxidation efficiency. From the measured emissions and the oxidation efficiency from the carbon shift method the base flux was calculated as the product of the volumetric emission and the efficiency. Consequently, no base fluxes could be calculated for grid fields without methane by this approach.

3. Methane Oxidation Tool (MOT)

The Methane Oxidation Tool (MOT) (Gebert et al., 2011c) is a simplified model approach to estimate methane oxidation rates in landfill cover soils. It factorizes a standard oxidation unit of 17.1 g CH₄ m⁻² d⁻¹ (equivalent to 6.2 kg CH₄ m⁻² a⁻¹ or 1 L m⁻² h⁻¹) given at conditions of 14% porosity, at a temperature of 20 °C and 6 kPa water potential. According to the prevailing conditions of soil temperature, air capacity (volumetric air content at field capacity (6 kPa suction or pF 1.8) and soil water potential (as pF-value = log water potential in the unit hPa), based on the known influence of these parameters on the process of methane oxidation, the standard oxidation unit is thereby corrected to a more realistic site specific factorized oxidation unit. The value for the standard oxidation unit is an empirical assumption made by the authors of the model based on literature and own data. In the following the factors are described briefly and the calculation for the factorized oxidation unit is given.

As every biochemical process, the methane oxidation rate is dependent on temperature. With increasing temperatures oxidation rates increase. Beyond the temperature optimum, in this case approximately 35 °C, the oxidation rate declines due to degeneration of proteins. The nature of the relationship is known from many studies (for a review see Scheutz et al., 2009). In the MOT the temperature factor can vary from 0.25 to 2.78 (hence modifying the standard oxidation unit from 25% to 278%). For each 5 °C step from 0 °C to 50 °C one factor is defined according to the known temperature-activity relationships (Fig. 3). With increasing temperatures oxidation rates increase.

With increasing air capacity, the diffusive flux of oxygen from the atmosphere into the soil increases. As two mol of oxygen are needed to oxidize one mol of methane, the diffusive oxygen ingress defines the soil's oxidation potential. The air capacity factor varies from 0.05 to 9.73 for porosities from 10% to 36% v/v with an increment of 2%. The relationship is based on the relation between porosity and diffusivity determined by Gebert et al. (2011a).

All biologically mediated process in the soil respond to the soil's water potential (or matric potential) as it defines the osmotic gradient between the soil and the soil organisms. The factor for soil water potential covers the range of water potentials from pF 1.8 (6 kPa) to pF 4.2 (1500 kPa) and assigns factors from one to zero with a step size of about pF 0.5 for each factor, based on the relationship determined by Gebert (2013). At water potentials lower than pF 1.8 (6 kPa) the water cannot drain freely and the soil is water logged, hence the methane oxidation rate declines due to limitations of diffusion of oxygen. At pF 1.8 (6 kPa) water supply for methanotrophic bacteria is optimal and air capacity pore space is fully available. At pF 4.2 (1500 kPa) it is too dry for methanotrophic bacteria so no oxidation will happen.

After identifying the factors they are multiplied with the standard oxidation potential (SOP) to derive the factorized oxidation potential (FOP) according to Eq. (2). This output is the expected site specific oxidation rate at the prevailing point in time for which the

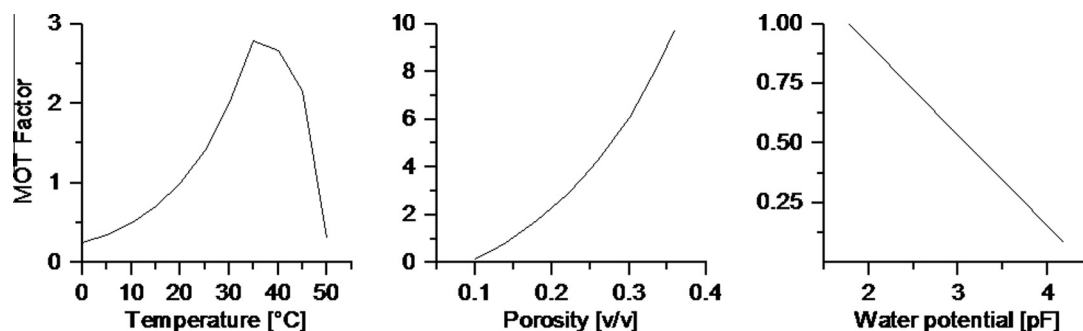


Fig. 3. MOT factors for temperature, porosity and water potential. Adapted from (Gebert et al., 2011c).

environmental conditions (temperature, air-filled porosity and water potential) are valid.

$$FOP = SOP * F_{temp} * F_{por} * F_{wp} \quad (2)$$

with

- FOP = factorized oxidation potential,
- SOP = standardized oxidation potential,
- F_{temp} = factor for influence of temperature,
- F_{por} = factor for influence of porosity,
- F_{wp} = factor for influence of water potential.

The model is available online in form of a spreadsheet and an explanatory document from <http://www.afvalzorg.nl/EN/About-us/Publications/Methane-oxidation.aspx>.

In the comment to the model it is proposed to use the input data on soil temperature, water potential and air capacity for the depth corresponding to the middle of the assumed oxidation horizon. As in the case of the investigated test field gas profiles indicate oxidation down to 1 m (data not shown), soil temperature and moisture data from the sensor set installed in 40 cm depth were chosen (details on sensors in Section 2.1). Water potential was calculated by applying the data on volumetric water content measured by the FDR probes to the water retention curve analyzed for the subsoil material.

Direct emissions are considered in the MOT as a cover type dependent share of the load to the cover that bypasses the oxidation layer through macropores such as cracks and hence does not take part in the methane oxidation process. Correction factors of 0.1 (i.e. 10% direct emissions) for permanent covers >100 cm thickness with a gas distribution layer and a porosity of over 20% up to 0.9 (i.e. 90% direct emissions) for daily covers or uncovered landfills are proposed. The assumption on the share of direct emissions from each cover type is based on field data on methane oxidation in Dutch landfills from *The Netherlands Organisation of Applied Scientific Research* (TNO). Still the database to derive a reliable relationship between cover type and share of direct emissions has to be broadened.

Instead of the air capacity, the actual air filled pore volume was used as input parameter here. It was derived subtracting the measured volumetric water content from the total porosity determined for the material.

4. Results and discussion

4.1. Variability of environmental conditions and corresponding model results

The temporal variability of the input parameters for the MOT prediction of the oxidation potential (air filled porosity, soil temperature and water potential) are displayed in Fig. 4. To account

for changes of the total pore volume due to settlement of the soil material over time and for uncertainties in the soil moisture measurement, the factor for air filled porosity is given for $\pm 5\%$ water content accounting for the moisture sensor accuracy given by the manufacturer and the experience of Röwer (2014) working with the same setup. A typical seasonal pattern can be seen for the temperature and moisture course with warm temperatures and dryer conditions in summer and moister and colder winters. The resulting input factors and the according factorized oxidation potential (FOP) are displayed as well. It can be seen that the variability in air filled porosity, determining the diffusive ingress of atmospheric oxygen, has the highest influence on the oxidation potential, followed by temperature. Hence, the water content of the soil is the crucial parameter, regulating the share of air filled pore volume. This was also found by Racher et al. (2013) for emissions from hot-spots on an old landfill in northern Germany. Soil moisture had an immediate influence on the emission intensity on the scale of hours and days while temperature fluctuations could explain a large share of the seasonal variability. The resulting estimated oxidation potential ranged from 20.6 to 92.7 g CH₄ m⁻² d⁻¹ with a mean of 44.6 and a standard deviation (SD) of 20.6 g CH₄ m⁻² d⁻¹.

4.2. Oxidation efficiency and rates

The oxidation efficiency from the mass balance method yielded efficiencies for the whole test field without a spatial resolution. The mean oxidation efficiency was 83.6% before (August 2012–July 2013) and 84.9% after reconstruction (February 2014–February 2015). The maximum average efficiency of the test field was 100% in June 2014 and the lowest performance was 48.1% in October 2012. The efficiencies and the loads and emissions of the entire field are given in Fig. 5. The oxidation efficiencies derived from the carbon shift method differ a bit. Mean oxidation efficiency was 75.3% while the maximum was 99.6% and the minimum 24.5% (Fig. 5). Both methods yield very similar results over most of the time. The temporal pattern reflects the expected influence of the environmental parameters. In the winter month characterized by lower temperatures and lower air filled porosity due to higher soil moisture content the efficiencies were lower than in the summer month. Major emissions occurred only in the winter month. The findings on the magnitude of the oxidation efficiency are in accordance with other studies (Capanema and Cabral, 2012; Scheutz et al., 2014) albeit the former was achieved at load up to 290 and 818 g m⁻² d⁻¹ and the latter at loads around 27 g m⁻² d⁻¹. Other studies found a somewhat lower oxidation efficiency of about 50% (Dever et al., 2011) at loads from 48 to 83 g m⁻² d⁻¹, hence comparable to the loads in this study.

The oxidation rates can be obtained if the amount of methane removed is related to units of area and time. In Fig. 5 oxidation rates calculated for the total test field are displayed, derived from the methane mass balance. The maximum rate was 41.2 g CH₄

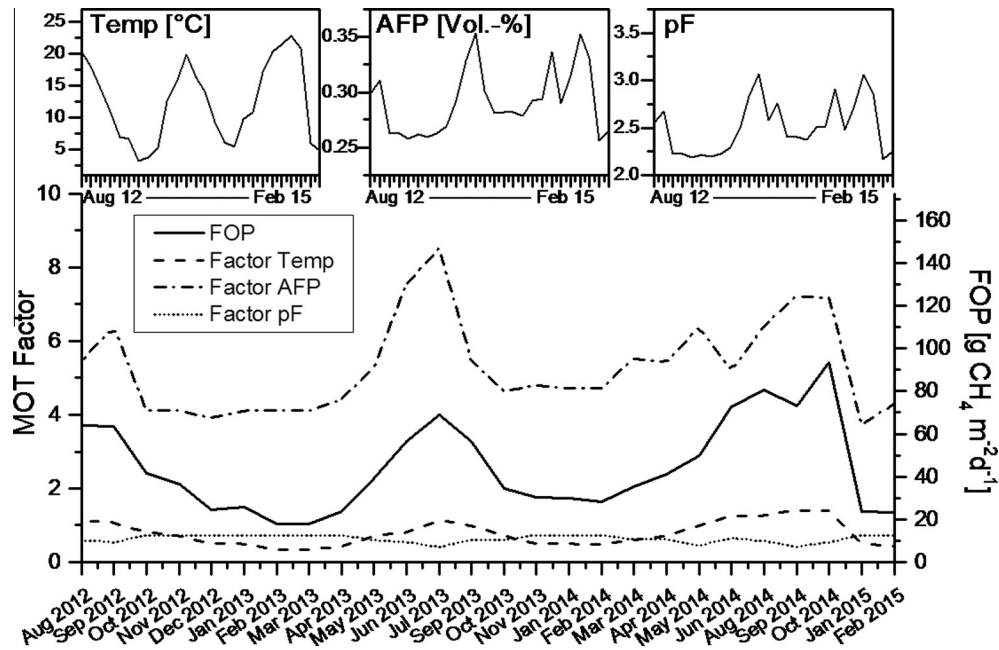


Fig. 4. MOT input parameters (top), factors (left y-axis) and resulting estimation of oxidation potential (right y-axis) (bottom). Temp = soil temperature in 40 cm depth, AFP = air filled porosity in 40 cm depth, pF = log water potential in 40 cm depth. FOP = factorized oxidation potential (model output).

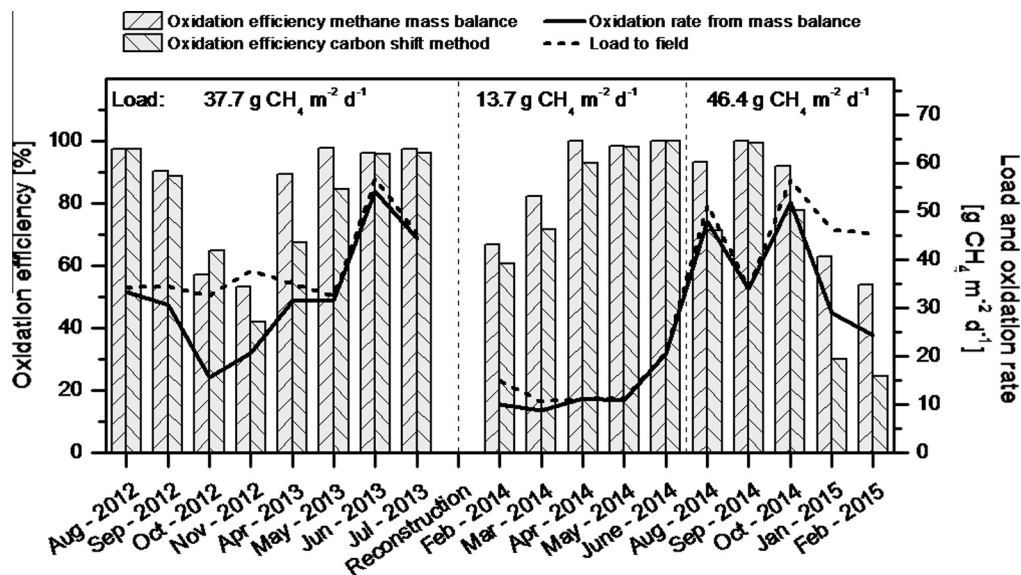


Fig. 5. Time course of oxidation efficiency from mass balance and carbon shift method and oxidation rate. Carbon shift efficiencies are averages over all grid fields. Oxidation rates are calculated from influx and mass balance efficiencies related to the test field area.

$\text{m}^{-2} \text{d}^{-1}$ and the minimum rate was $10.3 \text{ g CH}_4 \text{ m}^{-2} \text{ d}^{-1}$. The load to the field in the investigation period varied between $10.3 \text{ g CH}_4 \text{ m}^{-2} \text{ d}^{-1}$ (March 14) and $56.7 \text{ g CH}_4 \text{ m}^{-2} \text{ d}^{-1}$ (June 13). The oxidation rates found are comparable to findings of other studies (overview at Sadasivam and Reddy, 2014; Scheutz et al., 2009). Average rates for a biowindow of $20.4 \text{ g CH}_4 \text{ m}^{-2} \text{ d}^{-1}$ were reported by Scheutz et al. (2011). Mei et al. (2015) found oxidation rate of $140\text{--}200 \text{ g CH}_4 \text{ m}^{-2} \text{ d}^{-1}$ in a green waste biocover. Extremely high rates up to $818 \text{ g CH}_4 \text{ m}^{-2} \text{ d}^{-1}$ are reported from Capanema and Cabral (2012) for a sand and compost biofilter. In contrast to the study presented here the afore-mentioned methane oxidation systems used compost material as filter substrate. Huber-Humer et al. (2011) showed that mature compost is a more effective filter bed material than mineral soil. The advantage of

mineral material is its mechanical long term stability which is not given for compost material which is microbially degradable (Jugnia et al., 2008). The achievable oxidation rate of a system depends not only on the used material setup and environmental conditions but also on the exposure to methane. Röwer et al. (2011) found a positive correlation between methane concentration in the soil of an old landfill and its methane oxidation capacity. They assumed that a low level exposure builds the potential for rapid population growth when the soil is exposed to higher loads. Gebert et al. (2003) showed that prolonged methane exposition of a biofilter increased its methane oxidation rates. In batch tests Gebert (2013) showed that repeated cycles of methane incubation and oxidation increased the soils methane oxidation rates. The final rates ($0.5\text{--}45 \mu\text{g CH}_4 \text{ g}_{\text{dw}}^{-1} \text{ h}^{-1}$) were dependent on the

incubation temperature while the asymptotic shape of the curve was similar for all incubation temperatures (4–37 °C). Measurement data from landfills in The Netherlands indicate that the oxidation rate increases with the load but deviating ever more from a 1:1 relationship until reaching a maximum at about 24 g CH₄ m⁻² d⁻¹ (Oonk and Boom, 1995). It has to be considered, that oxidation rates in this study have been restricted over most of the time by the applied load hence the potential of the cover was not challenged and maybe not fully built up.

4.3. Spatial variability of oxidation efficiency

Using the carbon shift method the oxidation efficiency could be computed on a grid field scale, using the relationship of carbon dioxide to methane in 1 m depth and in the emitted gas. Two exemplary campaigns were selected for analysis of spatial variability, reflecting typical summer and winter conditions (September 2014 and February 2015, Fig. 6). In September 2014 emission measurements were performed on all grid fields (except row no. 10) and in February 2015 on about two thirds of the grid fields. Due to lower oxidation efficiencies in winter, emissions are higher and spatial patterns can be seen more clearly.

It could be shown that the oxidation efficiency was heterogeneous on a spatial scale. Always some grid fields showed oxidation efficiencies close to or 100%. The lowest oxidation efficiencies were always found on the upper slope and the lateral limits of the catchment. This was attributed to the combined use of the capillary barrier as gas distribution layer and drainage water control. If percolation water is discharged into the capillary barrier a saturated water seam forms at the interface between the capillary block and the capillary layer, reducing the diffusivity and gas permeability. As water accumulates along the path length, i.e. the downslope path, this effect becomes more pronounced in downslope positions and in the moister seasons. Vice versa, it is likely

that the capillary fringe forming in the capillary layer just above the capillary block is less continuous the more upslope it is. This effect was also observed by (Tétrault and Cabral, 2013). Thus, the gas that distributes in the capillary block/gas distribution layer can enter the methane oxidation layer passing the capillary layer more easily in the upslope area. This results in an uneven load to the methane oxidation layer with peak loads upslope. Consequently, the upslope area receives a load that is higher than the nominal load derived from the bulk base flux and the base area. This can lead to an overload while some parts downslope receive less than they could oxidize and thus cannot exploit their full oxidation potential. The heterogeneous emission pattern was found before and after the reconstruction works albeit the heterogeneity was less pronounced after the reconstruction. This was attributed to the compaction (from 1.34 to 1.39 g cm⁻³) of the methane oxidation layer that was realized during the reconstruction which yielded a higher difference of gas conductivities between gas distribution layer and methane oxidation layer. This led to a more homogeneous distribution of the gas within the gas distribution system, corroborated by gas composition measurements using gas probes in 1 m depth on grid field scale resolution (Fig. 7), see also Section 4.4. This points to the importance of carefully balanced porosities of the individual layers of the MOS to receive a maximum evenness of gas flow. Furthermore, the combination of gas distribution systems and capillary barrier seems problematic with respect to homogeneous gas distribution. This was confirmed by Wawra and Holfelder (2003) who found a reduction of gas conductivity along a hill slope of two orders of magnitude as a result of capillary effects. In German recommendation guidelines for MOS it is emphasized that the difference in gas permeability between gas distribution layer and methane oxidation layer should be at least two orders of magnitude while on the other hand a capillary barrier effect should be avoided (LAGA Ad-hoc AG "Deponietechnik", 2011).

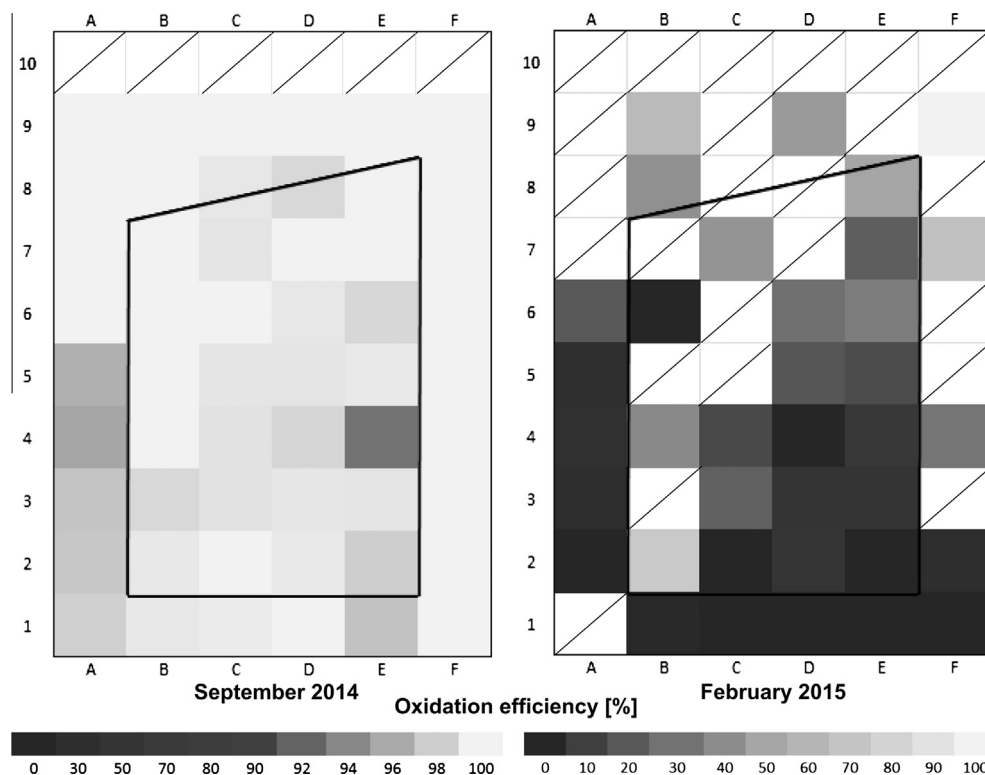


Fig. 6. Oxidation efficiency on grid field scale. Note the different color scales for September 2014 and February 2015. Black line: border of catchment. Diagonal line: no data. Lower margin is upslope.

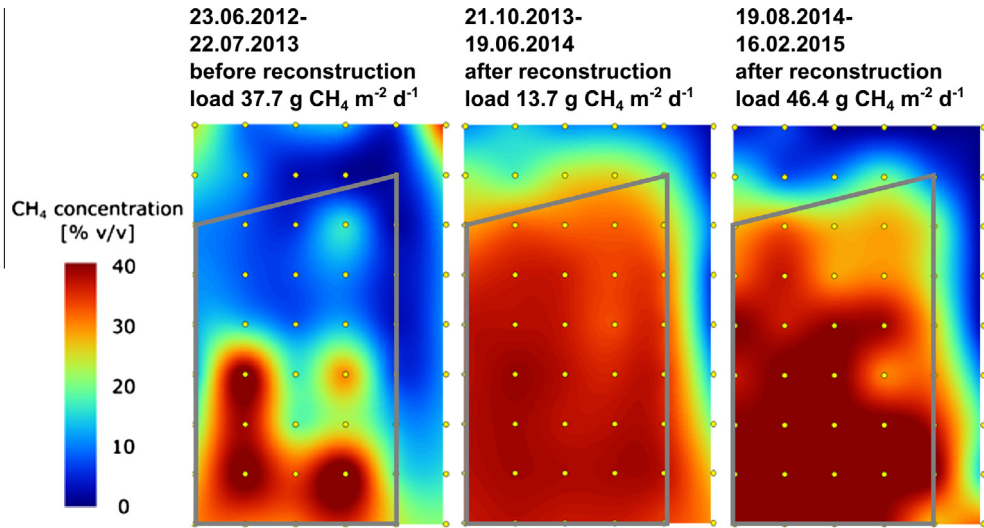


Fig. 7. Mean methane concentration in 1 m soil depth for three monitoring intervals. Lower margin of the image is upslope. Black line: catchment. Yellow dots: gas probes. Yellow dot at the bottom on the left is gas probe A1, highest on the right is F9.

4.4. Model predictions and measurements- resolving the test field to grid field scale

In soil gas phase surveys it was found that the gas was not evenly distributed at the base of the test field and subsequently also not in more shallow depths. If gas distribution is spatially heterogeneous, the average bulk load to the whole test field does not represent the load to each individual grid field, i.e. the scale on which the chamber measurements were conducted. The calculation of the base flux from grid field scale data on emission and oxidation efficiency was an attempt to resolve the spatial variability of the load. The resulting grid field scale data set was used (1) to study the response of the test field to changing seasonal conditions and (2) to broaden the data basis against which model predictions were compared.

To study the response of the test field to changing seasonal conditions the relationship between base flux and oxidation rate and the resulting oxidation efficiency was examined in-depth for two exemplary campaigns (same campaigns as in Fig. 6). The data is plotted in Fig. 8. Each circle represents one grid field that was emissive in the relevant campaign. The ambient conditions are given in Fig. 4.

In September 2014 soil temperature was 22.8 °C and air filled porosity was 35%. Under these conditions most of the methane was oxidized in the soil. A higher base flux coincided with higher oxidation rates. All the measurements showed a base flux – oxidation rate – ratio of close to one, i.e. all supplied methane was oxidized. In this state the system was loaded below its potential.

In February 2015 at only 4.9 °C and an air filled porosity of 27% most data points concentrated between the 50% and the 10% efficiency isoline. High efficiencies occurred only at low base fluxes. With increasing base flux the rate increased as well but deviated ever more from the 100%-line the higher the base flux became.

Comparing the base fluxes with the oxidation rates on grid field scale revealed different scenarios depending on seasonal conditions. The achieved rates were about one order of magnitude lower in the winter campaign. In contrast to the unique relation between base flux and oxidation rate close to the 100% isoline in September 2014, in February 2015 in different grid fields a different share of similar base fluxes was oxidized under similar environmental conditions. The ambient conditions seemed to (1) change the achievable oxidation rate and (2) influence the heterogeneity of the base flux distribution. The reduced oxidation rates in winter were to be expected due to the influence of colder temperatures

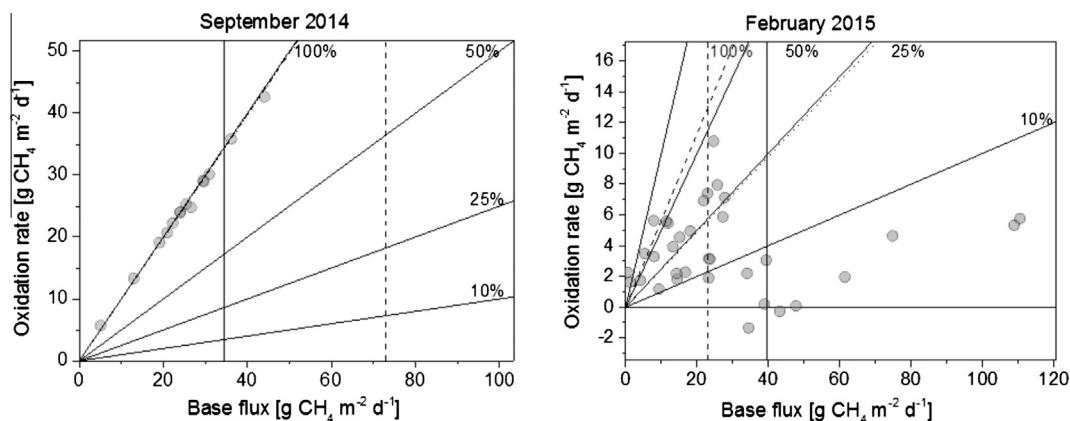


Fig. 8. Relationship between base flux, oxidation rate and oxidation efficiency on grid field scale. Isolines for 10, 25, 50 and 100% oxidation are given. Dashed isoline: efficiency from mass balance; dotted isoline: efficiency from carbon shift method. Solid vertical line: average load to test field; dashed vertical line: factorized oxidation potential. Note the different x and y axes.

(Scheutz et al., 2009) and reduced air-filled pore space due to increased precipitation and decreased evapotranspiration in the colder season. Moreover, the moister soil and increased discharge of drainage water into the capillary layer in the February 2015 campaign presumably impeded a homogenous horizontal distribution of the supplied base load. From the known water retention curves it could be calculated that the increased soil moisture resulted in decrease of the soil water tension from pF 3.06 to 2.25 (equaling 115 kPa to 18 kPa), compared to the September 2014 campaign. The water-free pore space available for gas transport was hence restricted to pores with an equivalent diameter of 2.6 μm , compared to 16.5 μm in September 2014. For winter conditions this indicates a blockage of the middle pores (0.2–10 μm diameter) leaving only the coarse pores > 16.5 μm diameter (pores > 10 μm are defined as coarse pores) available for gas transport while under summer conditions also most of the middle pores were water-free. If only the coarser pores including cracks, root channels and animal burrows are available for gas transport it becomes less homogeneous (Allaire et al., 2008; Giani et al., 2002). The same amount of gas flowing through a smaller pore volume results in higher rates of gas transport per unit area which results in lower turnover rates and hence higher emissions. This was also found by Dever et al. (2011). Most likely this is due to impediment of oxygen ingress due to an increased flow rate of landfill gas from below (Rachor et al., 2011), restricting the oxidation process to the upper soil layers.

The predictions of the MOT were compared against the base flux data on grid field scale. In Fig. 9 the range of base fluxes to the individual grid fields and the load to and emissions from the whole test field are plotted along with the model-derived oxidation potential (FOP). Emissions occur when the oxidation rate is below the load (hatched area), that is in autumn/winter 2012, spring 2013, late winter 2014 and autumn/winter 2014/2015. The load exceeds the FOP only in November 2012, April 2013 and January and February 2015. The range of the base fluxes was significantly higher before than after the reconstruction. This indicates a more homogeneous distribution of the load. As base fluxes could be calculated only for emissive fields, loads to grid fields with 100% oxidation are lacking in the boxplot graph. Peak fluxes were

higher before the reconstruction. Larger emissions occurred only when base fluxes were higher than the FOP, indicating an overload. The MOT predictions for “high potential times”, i.e. for dryer and warmer conditions could not be challenged because the loads to the test field were not that high. In winter, especially with the optimized gas distribution after the reconstruction, the predicted rates seemed to be realistic. Findings from laboratory column studies often indicate higher rates which can be explained by higher applied loads and optimal conditions of substrate supply as well as favorable temperatures (overview in Scheutz et al., 2009).

The MOT assumes a share of the load to bypass the MOS as direct emissions. The magnitude of this share should depend on the cover type. For daily covers (<30 cm, no gas distribution layer) or uncovered sites 90% are assumed to emit directly, for temporary covers (>30 cm, no gas distribution layer) depending on their porosity 60–80% and for final covers (>100 cm, gas distribution layer) 10–50% are assumed, again depending on the porosity. However, the data clearly show that no fixed share of the load is converted into direct emissions. On annual average 16% of the injected methane could not be oxidized. That is in the order of magnitude proposed by the MOT for direct emissions for a final cover with a porosity over 20%. The porosity of the examined system was about 20%. Direct emissions are meant to be emissions through cracks and animal burrows or other shortcuts bypassing the methane oxidation system. Bergamaschi et al. (1998) attributed 70% of the methane transport into the atmosphere to direct emissions from a non-optimized cover. For this study it could not be shown to which extent direct emission happened. Surface screenings of methane and carbon dioxide concentrations (results not shown) did show spots with a $\text{CO}_2\text{-CH}_4$ ratio similar to the supplied landfill gas, indicating the existence of direct emission pathways. However, such spots could not be identified in all surface screening campaigns. Rachor (2012) and Röwer et al. (2016) showed that surface concentration data cannot be used to calculate emissive fluxes. No flux data was acquired for the identified spots, making a quantification of the emission through these spots and hence the assessment of the share of direct emissions impossible. Based on the fact that locations of direct emissions, characterized by a $\text{CO}_2\text{-CH}_4$ ratio similar to the landfill gas, were not permanently

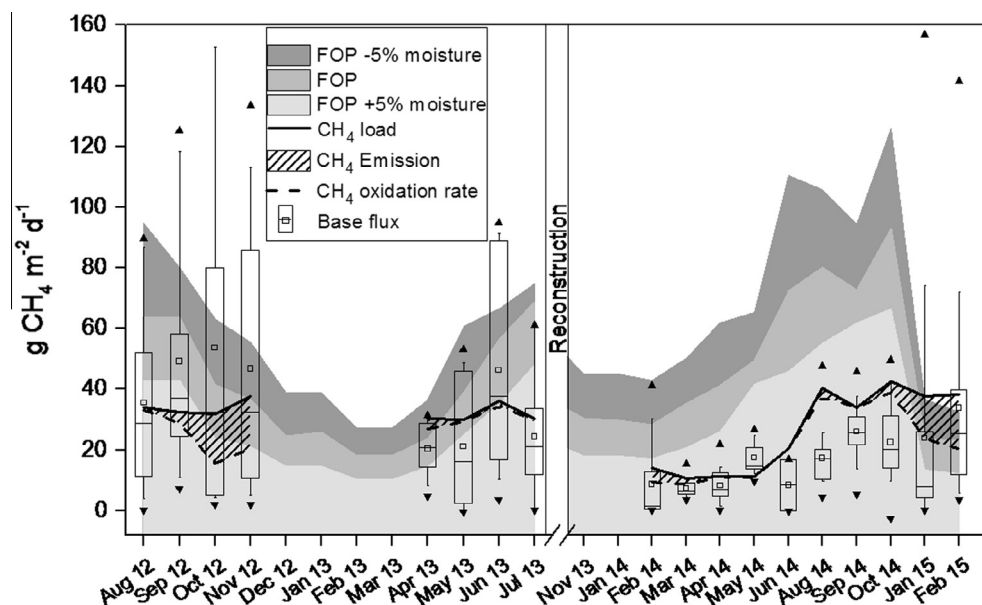


Fig. 9. MOT predictions for factored oxidation potential (FOP) (gray area), measured load (solid line), oxidation rate (dashed line), resulting emissions (hatched area) and calculated base flux in 1 m depth (boxplot) (Box: 25–50%, square: arithmetic mean, whiskers: 10–90%, triangles: min/max). For the FOP the effect of $\pm 5\%$ moisture content is indicated.

it is assumed that the share of direct emissions via bypasses is likely to be smaller than suggested by the MOT, confirming the conservative assumptions of the model. The detected methane emissions are more likely explained by a sporadic overloading of the test field.

5. Conclusions

From this study it can be concluded that given a homogeneous gas distribution and a moderate load methane oxidation systems are highly efficient systems to mitigate landfill gas emissions for the period of aftercare when landfill gas usage or flaring are no longer possible or viable. The oxidation potential estimation using the Methane Oxidation Tool seems promising albeit the upper range could be challenged only at very few occasions because the loading rate mostly stayed below the predicted oxidation potential. Further field trials involving higher methane loads challenging the predicted rates would further increase the validation of the Methane Oxidation Tool prognosis. The combined use of the capillary barrier as gas distribution layer resulted in heterogeneous gas flux to the cover. If the combination of these functions is aspired, the increased load to the upslope area has to be considered in the dimensioning of the system. No fixed share of direct emissions could be confirmed, yet the annual average assumed by the Methane Oxidation Tool for the respective cover type more or less reflected the measured emissions. Further investigations could address the differentiation between direct emissions and emissions resulting from an overload. A spatially heterogeneous emission pattern was found on a scale of 17 m². It was shown that the spatial pattern of emissive fluxes remained constant over the observation period while its magnitude intensified as overall emissions increased. This shows that the spatial gas transport patterns in the methane oxidation cover remained stable over time and that the magnitude of oxidation and hence of emission fluxes is modulated by the seasonal variation of the methane oxidation capacity.

Acknowledgement

The authors thank all colleagues and students for the good spirit over the long working hours in the field and thereafter. Special thanks go to Volker Kleinschmidt who contributed substantially to the technical implementation of the measurement equipment and to get the thinking out of the box again.

References

- Allaire, S.E., Lafond, J.A., Cabral, A.R., Lange, S.F., 2008. Measurement of gas diffusion through soils: comparison of laboratory methods. *J. Environ. Monit.* 10 (11), 1326. <http://dx.doi.org/10.1039/b809461f>.
- Bergamaschi, P., Lubina, C., Königstedt, R., Fischer, H., Veltkamp, A.C., Zwaagstra, O., 1998. Stable isotopic signatures ($\delta^{13}\text{C}$, δD) of methane from European landfill sites. *J. Geophys. Res.* 103 (D7), 8251. <http://dx.doi.org/10.1029/98JD00105>.
- Bogner, J., Abdelrafie Ahmed, M., Diaz, C., Faaij, A., Gao, Q., Hashimoto, S., Mareckova, K., Pipatti, R., Zhang, T., 2007. *Waste Management*. In: Metz, B., Davidson, O.R., Bosch, P.R., Dave, R., Meyer, L.A. (Eds.), *Climate Change 2007: Mitigation. Contribution of Working Group III to the Fourth Assessment Report of the Intergovernmental Panel on Climate Change*, Cambridge, UK and New York, NY, USA.
- Bogner, J., Meadows, M., Czepiel, P., 1997. Fluxes of methane between landfills and the atmosphere: natural and engineered controls. *Soil Use Manage.* 13 (s4), 268–277. <http://dx.doi.org/10.1111/j.1475-2743.1997.tb00598.x>.
- Capanema, M.A., Cabral, A.R., 2012. Evaluating methane oxidation efficiencies in experimental landfill biocovers by mass balance and carbon stable isotopes. *Water Air Soil Pollut.* 223 (9), 5623–5635. <http://dx.doi.org/10.1007/s11270-012-1302-6>.
- Christophersen, M., Kjeldsen, P., Holst, H., Chanton, J.P., 2001. Lateral gas transport in soil adjacent to an old landfill: factors governing emissions and methane oxidation. *Waste Manage. Res.* 19 (6), 595–612. <http://dx.doi.org/10.1177/0734242X0101900616>.
- Dever, S.A., Swarbrick, G.E., Stuetz, R.M., 2011. Passive drainage and biofiltration of landfill gas: results of Australian field trial. *Waste Manage. (New York, N.Y.)* 31 (5), 1029–1048. [10.1016/j.wasman.2010.10.026](http://dx.doi.org/10.1016/j.wasman.2010.10.026).
- FAO, 2014. *World Reference Base for Soil Resources 2014: International Soil Classification System for Naming Soils and Creating Legends for Soil Maps*. FAO, Rome, Online-Resource.
- Gebert, J., Gröngroft, A., Miehllich, G., 2003. Kinetics of microbial landfill methane oxidation in biofilters. *Waste Manage.* 23 (7), 609–619. [http://dx.doi.org/10.1016/S0956-053X\(03\)00105-3](http://dx.doi.org/10.1016/S0956-053X(03)00105-3).
- Gebert, J., Gröngroft, A., Pfeiffer, E.-M., 2011a. Relevance of soil physical properties for the microbial oxidation of methane in landfill covers. *Soil Biol. Biochem.* 43 (9), 1759–1767. <http://dx.doi.org/10.1016/j.soilbio.2010.07.004>.
- Gebert, J., Röwer, I.U., Scharff, H., Roncato, C.D.L., Cabral, A.R., 2011b. Can soil gas profiles be used to assess microbial CH₄ oxidation in landfill covers? *Waste Manage.* 31 (5), 987–994. <http://dx.doi.org/10.1016/j.wasman.2010.10.008>.
- Gebert, J., Scharff, H., Huber-Humer, M., Oonk, H., 2011c. Methane Oxidation Tool – An Approach to Estimate Methane Oxidation on Landfills <http://www.afvalzorg.nl/EN/About-us/Publications/Methane-oxidation.aspx>.
- Gebert, J., 2013. Microbial oxidation of methane fluxes from landfills. *Hamburger Bodenkundliche Arbeiten*.
- Geck, C., Röwer, I.U., Kleinschmidt, V., Scharff, H., Gebert, J., 2016. Design, validation and implementation of a novel accumulation chamber system for the quantification of CH₄ and CO₂ emissions from landfills. Technical Report.
- Giani, L., Bredenkamp, J., Eden, I., 2002. Temporal and spatial variability of the CH₄ dynamics of landfill cover soils. *Z. Pflanzenernähr. Bodenkd* 2002 (165), 205–210.
- Huber-Humer, M., Tintner, J., Böhm, K., Lechner, P., 2011. Scrutinizing compost properties and their impact on methane oxidation efficiency. *Waste Manage. (New York, N.Y.)* 31 (5), 871–883. [10.1016/j.wasman.2010.09.023](http://dx.doi.org/10.1016/j.wasman.2010.09.023).
- Jugnia, L.-B., Cabral, A.R., Greer, C.W., 2008. Biotic methane oxidation within an instrumented experimental landfill cover. *Ecol. Eng.* 33 (2), 102–109. <http://dx.doi.org/10.1016/j.ecoleng.2008.02.003>.
- LAGA Ad-hoc AG “Deponietechnik”, 2011. *Bundeseinheitlicher Qualitätsstandard 7–3 Methanoxidationsschichten in Oberflächenabdichtungssystemen*.
- Mei, C., Yazdani, R., Han, B., Mostafid, M.E., Chanton, J.P., VanderGheynst, J., Imhoff, P., 2015. Performance of green waste biocovers for enhancing methane oxidation. *Waste Manage. (New York, N.Y.)* 39, 205–215. [10.1016/j.wasman.2015.01.042](http://dx.doi.org/10.1016/j.wasman.2015.01.042).
- Oonk, J., Boom, A., 1995. *Landfill Gas Formation, Recovery and Emission: TNO-Report Nr. 410 100 036*, Apeldoorn, The Netherlands.
- Park, S., Lee, C.-H., Ryu, C.-R., Sung, K., 2009. Biofiltration for reducing methane emissions from modern sanitary landfills at the low methane generation stage. *Water Air Soil Pollut.* 196 (1–4), 19–27. <http://dx.doi.org/10.1007/s11270-008-9754-4>.
- Rachor, I., Gebert, J., Gröngroft, A., Pfeiffer, E.-M., 2011. Assessment of the methane oxidation capacity of compacted soils intended for use as landfill cover materials. *Waste Manage.* 31 (5), 833–842. <http://dx.doi.org/10.1016/j.wasman.2010.10.006>.
- Rachor, I., 2012. *Spatial and Temporal Patterns of Methane Fluxes on Old Landfills: Processes and Emission Reduction Potential*. *Hamburger Bodenkundliche Arbeiten*, Hamburg.
- Rachor, I.M., Gebert, J., Gröngroft, A., Pfeiffer, E.-M., 2013. Variability of methane emissions from an old landfill over different time-scales. *Eur. J. Soil Sci.* 64 (1), 16–26. <http://dx.doi.org/10.1111/ejss.12004>.
- Röwer, I.U., Geck, C., Gebert, J., Pfeiffer, E.-M., 2011. Spatial variability of soil gas concentration and methane oxidation capacity in landfill covers. *Waste Manage.* 31 (5), 926–934. <http://dx.doi.org/10.1016/j.wasman.2010.09.013>.
- Röwer, I.U., 2014. Reduction of methane emissions from landfills: processes, measures and monitoring strategies. *Hamburger Bodenkundliche Arbeiten*.
- Röwer, I.U., Streese-Kleeberg, J., Scharff, H., Pfeiffer, E.-M., Gebert, J., 2016. Optimized landfill biocover for CH₄ oxidation II: Implications of spatially heterogeneous fluxes for monitoring and emission prediction. *Environ. Eng.* 10 (submitted for publication).
- Sadasivam, B.Y., Reddy, K.R., 2014. Landfill methane oxidation in soil and bio-based cover systems: a review. *Rev. Environ. Sci. Bio/Technol.* 13 (1), 79–107. <http://dx.doi.org/10.1007/s11157-013-9325-z>.
- Scheutz, C., Fredenslund, A.M., Chanton, J.P., Pedersen, G.B., Kjeldsen, P., 2011. Mitigation of methane emission from Faxe landfill using a biowindow system. *Waste Manage. (New York, N.Y.)* 31 (5), 1018–1028. [10.1016/j.wasman.2011.01.024](http://dx.doi.org/10.1016/j.wasman.2011.01.024).
- Scheutz, C., Kjeldsen, P., 2004. Environmental factors influencing attenuation of methane and hydrochlorofluorocarbons in landfill cover soils. *J. Environ. Qual.* 33, 72–79.
- Scheutz, C., Kjeldsen, P., Bogner, J.E., de Visscher, A., Gebert, J., Hilger, H.A., Huber-Humer, M., Spokas, K., 2009. Microbial methane oxidation processes and technologies for mitigation of landfill gas emissions. *Waste Manage. Res.* 27 (5), 409–455. <http://dx.doi.org/10.1177/0734242x09339325>.
- Scheutz, C., Pedersen, R.B., Petersen, P.H., Jørgensen, Jørgen Henrik Bjerre, Ucendo, Inmaculada Maria Buendia, Mønster, J.G., Samuelsson, J., Kjeldsen, P., 2014. Mitigation of methane emission from an old unlined landfill in Klintholm, Denmark using a passive biocover system. *Waste Manage. (New York, N.Y.)* 34 (7), 1179–1190. [10.1016/j.wasman.2014.03.015](http://dx.doi.org/10.1016/j.wasman.2014.03.015).
- Stein, V.B., Hettiaratchi, J.P.A., 2001. Methane oxidation in three Alberta soils: influence of soil parameters and methane flux rates. *Environ. Technol.* 22 (1), 101–111. <http://dx.doi.org/10.1080/09593332208618315>.

- Teclé, D., Lee, J., Hasan, S., 2009. Quantitative analysis of physical and geotechnical factors affecting methane emission in municipal solid waste landfill. *Environ. Geol.* 56 (6), 1135–1143. <http://dx.doi.org/10.1007/s00254-008-1214-3>.
- Tétrault, P., Cabral, A.R., 2013. Non-uniform distribution of biogas under a biocover due to capillary barrier effect: case studies. *Geo Montreal*.
- Wawra, B., Holfelder, T., 2003. Development of a landfill cover with capillary barrier for methane oxidation – the capillary barrier as gas distribution layer. In: *Proceeding Sardinia, Ninth International Waste Management and Landfill Symposium*.